Advances in Artificial Intelligence and Machine Learning; Research 6 (1) 5092-5109 Received 17-11-2025; Accepted 19-02-2026; Published online 26-02-2026

Glaucoma Diagnosis via Advanced Retinal Image Processing and V-RACNet Classification

V. Vijaya Madhavi madhavikrishnat@klh.edu.in
Research Scholar, Department of CSE, Koneru Lakshmaiah Education Foundation Hyderabad, Telangana, India.

P Lalitha Surya Kumari vlalithanagesh@gmail.com
Professor, Department of CSE, Koneru Lakshmaiah Education Foundation Hyderabad, Telangana, India

Corresponding Author: P Lalitha Surya Kumari

Abstract

The proposed paper presents a general architecture of processing context in glaucoma diagnosis, entailing steps such as image preprocessing to the classification with the new V-RACNet model. The initial stages involve image resizing, removal of the green plane, and enhancement of blood vessels extraction by morphological operations and thinning. Focal regions and features extraction of the fovea regions including GLCM texture features and statistical properties are identified through a clustering algorithm (K-means). The glaucoma detector trained on samples of 1114 samples of DRIVE database with 650 normal samples and 464 glaucomatous samples (Low-Tension Glaucoma or Angle-Closure Glaucoma). The dataset is separated into two portions, training (70%, 779 samples) and testing (30%, 335 samples) to determine the model performance and ability to generalize its performance on new data. Further on, a V-RACNet model is constructed, and trained on a labelled database, and tested to classify glaucoma. The proposed method has remarkably high accuracy (99.32%), sensitivity (99.42%), specificity (98.58%), and precision (99.26%) which indicates that it can be a powerful tool because of its automatization capabilities in glaucoma diagnosis.

Keywords: Glaucoma diagnosis, Retinal images, Image preprocessing, V-RACNet model, Blood vessel extraction, Morphological Operations.

1. INTRODUCTION

Glaucoma is an age-related disease and therefore, is of particular concern when dealing with older populations [1–3]. There are two typical forms of glaucoma Low-Tension Glaucoma (LTG) and Angle-Closure Glaucoma (ACG) [4, 5]. Normal-tension glaucoma, or LTG, is characterized by defects of the optic nerve and loss of visual field though the intraocular pressure is statistically normal [6, 7]. On the contrary, ACG is characterized by the abrupt or slow shutting of the drainage angle of the eye, which leads to elevated IOP [8]. It is important to learn the distinguishing characteristics [9]. Due to the asymptomatic nature of glaucoma in its early stages, routine eye check-ups are very

Citation: Vijaya Madhavi and P Lalitha Surya Kumari. Glaucoma Diagnosis via Advanced Retinal Image Processing and V-RACNet Classification. **Advances in Artificial Intelligence and Machine Learning.** 2026;6(1):283. https://dx.doi.org/10.54364/AAIML.2026.61283

important in the process of detecting individuals at risk [10]. The problem can be greatly managed with early treatment that is either in form of medication or surgery [11–13]. In the early detection of glaucoma, ML and DL methods have been demonstrated in the analysis of the complex medical data, including retinal images [14]. In addition, the incorporation of ML and DL methods in glaucoma diagnostics can help simplify the procedure because it offers precise and timely evaluations that are essential in the appropriate clinical decision-making [15–17].

The methodology shows how glaucoma diagnosis is done in a complete manner, sequentially resizing and deriving the green plane of the retinal images, deriving blood vessels and using morphological operations and thinning to better detect vessel edges. The GLCM features obtained through a clustering algorithm to identify the fovea areas and extract features are useful information concerning vessel texture and patterns. The statistical characteristics like mean and entropy of fovea regions enhance the diagnostic capacity. Markedly, V-RACNet model, which is trained on a labeled database, is a new contribution as it correctly classifies the input images as either normal healthy eyes, low-tension glaucoma, or angle-closure glaucoma.

The study article aims at offering an in-depth analysis of glaucoma detection, classification. Context importance of early glaucoma detection is described in the introduction (Section 1). It presents the objectives of the research, and the necessity of the use of advanced methods to resolve this acute health issue. Section 2 performs a comprehensive literature review including such crucial issues as glaucoma overview and available detection techniques. Section 3 provides the proposed system and the novel V-RACNet model, which clarifies the step-by-step approach of the image preprocessing to extracting the features, and lastly Glaucoma classification. Section 4 will show the results and discussion which will show processed images and evaluate the performance of the system based on the main metrics. Section 5 sums up the paper by concluding on the findings, highlighting the contributions the proposed system.

2. LITERATURE SURVEY

This is a literature review which forms the foundation on which the research can be conducted. Shinde [18], used a glaucoma. Separating the optic disc region and the optical cup was done using the U-Net architecture, and this is a major step in correctly discovering the signs of glaucoma. Sreng et al. [19], have presented an automatic Glaucoma detection scheme in another study. In 2023, Shoukat et al. [20], reported a way of diagnosing glaucoma automatically using retinal images. These works are transforming the glaucoma diagnosis landscape and prove the usefulness of deep learning models and various imaging methods. Proposed System (Explanation of modules preprocessing stage, Feature Extraction stage, Detection and Classification stage)

Based on FIGURE 1, it can be proposed that the proposed system represents an end-to-end pipeline of the concerned research processing, The V-RACNet is constructed and trained on a labelled database to distinguish between different types of glaucoma. The discussion on the above methodology with their equations is now discussed.

Displayed image: $f(x, y)$

$$\text{Resized image: } g(x, y) = f\left(\frac{x}{a}, \frac{y}{b}\right) \tag{1}$$

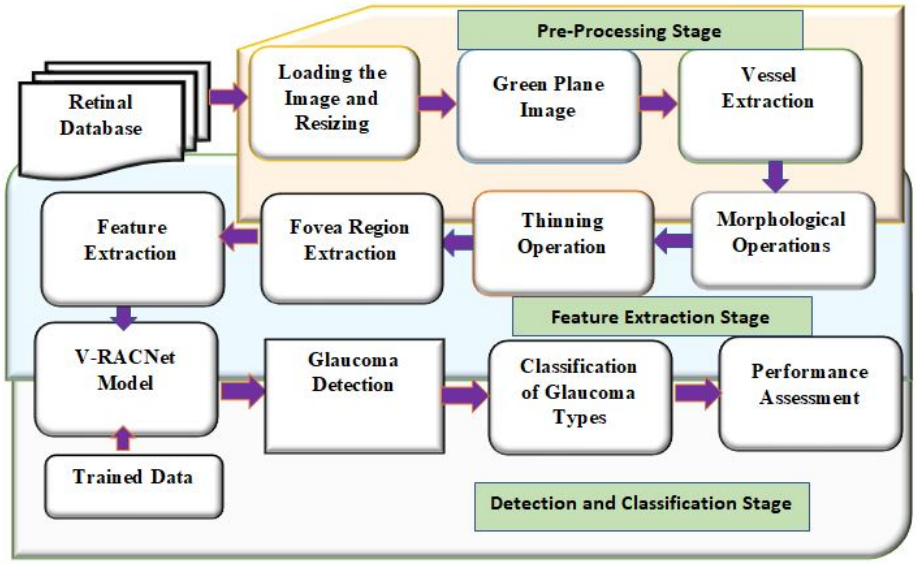

Figure 1: Proposed Glaucoma detection and Classification System

Factors Resizing factors are a,b. The green plane extraction may be expressed as

$$h(x, y) = f_g(x, y) \tag{2}$$

Resized extracted image:

$$i(x, y) = h\left(\frac{x}{c}, \frac{y}{d}\right) \tag{3}$$

where c,d scaling factors are scaled to 512X512 pixels. Altogether the entire transformation may be expressed as follows:

$$i(x, y) = f_g\left(\frac{x}{a}, \frac{y}{b}\right)\left(\frac{x}{c}, \frac{y}{d}\right) \tag{4}$$

The blood vessels are picked off the green plane of the input image. The methods of extracting blood vessels are important in diagnosing and treating diseases affecting the eyes. The extraction of the blood vessels may be symbolized.

$$j(x, y) = BloodVesselExtraction(i(x, y)) \tag{5}$$

where Blood Vessel Extraction is a procedure which pulls out blood vessels. The morphological operations like dilation, erosion and thresholding are employed to enhance vessel performance. k(x,y) is an image which is obtained after morphological operations. The operations are expressed as

$$k(x, y) = Dilation(Erosion(Threshold(j(x, y)))) \tag{6}$$

Threshold is a function which transforms the pixel intensities to binary values, where as Dilation and Erosion are morphological functions. Thinning is then done after morphological operations have been made to improve the edge detection of the vessel. l(x,y) is thinned vessel image. The thinning is done to enhance vessel edge detection. The image of the vessel that comes out appears in the Interface ready to conduct the research.

$$l(x, y) = Thinning(k(x, y)) \tag{7}$$

The input image is extracted into focal regions by use of a clustering algorithm (K-means). We transform this image into feature vectors X of dimension p x 1 , where $p = m \times n$ and each feature vector represent the intensity value of a pixel.

$$X = \{x1, x2, \ldots, xp\} \tag{8}$$

x i is the intensity value of the i th pixel. The centroids are enlarged using K.

$$C = \{c1, c2, \ldots, cK\} \tag{9}$$

where the centroid is a value of intensity. Given the pixel intensity xi, compute the distance between each centroid intensity cj and place it in the cluster, Sj.

$$Sj = \{\mathbf{x}i \; such \; that \; |\mathbf{x}i - \mathbf{c}j| \leq |\mathbf{x}i - \mathbf{c}k| \; for \; all \; k \; \neq j\} \tag{10}$$

$$\mathbf{c}j = \frac{1}{Sj} \sum_{Xi \in Sj} Xi \ldots\ldots\ldots\ldots\ldots\ldots\ldots\ldots \tag{11}$$

Repeat the above steps related to equations (8) to (11) until convergence conditions are achieved e.g., no centroid change of any significance is obtained. Once convergence has been attained, there are K clusters, each having the pixel intensity xi. GLCM is a matrix which depicts the distribution of co-occurring pixel values at a given offset or distance in an image. We will identify the image of the vessel as Ivessel m n. GLCM is computed using a number of determined properties, including distance, angle.

GLCM(i,j) is the co-occurrence matrix and i and j denote gray levels. GLCM is usually computed at a given offset d and a given angle θ.

$$GLCM(i,j) = \sum p = 1m \sum q = 1n\delta(Ivessel(p,q), i) \cdot \delta(Ivessel(p + \Delta x, q + \Delta y), j) \ldots\ldots \tag{12}$$

Extracted features of mean and entropy are obtained on the fovea regions to communicate the statistical characteristics. Mean feature is a measure of the average value of pixel value in the fovea area. It is calculated as:

$$Mean = \frac{1}{N} \sum_{i=1}^{N} I_{fovea}(i) \tag{13}$$

Entropy is used to quantify the randomness or uncertainty of intensity values of pixels in the fovea region. It is calculated as:

$$Entropy = -\sum_{i=1}^{L} p_i \log_2 p_i \tag{14}$$

L is the intensity levels in the fovea region and pi is the likelihood of occurrence fovea. Where D is the current database which holds labelled images of normal healthy eyes, low-tension glaucoma and angle-closure glaucoma. Where V-RACNet(x) is a model that is fed with input x producing a result.

$$L = -\frac{1}{N} \sum_{i=1}^{N} yilog(V - RACNet(xi)) + (1 - yi)log(1 - V - RACNet(xi)) \tag{15}$$

where N - aggregate number of training samples. After training and evaluating the model, it can be applied to classify according to their type of glaucoma.

$$Prediction(x) = V - RACNet(x) \tag{16}$$

3. PROPOSED MODEL

V-RACNet is a new algorithm of detecting glaucoma that integrates the advantages of VGG19 and recurrent neural networks (RNNs).V-RACNet This is an advanced method of glaucoma detection, which only addresses the detection and classification stages without extracting new features, except those obtained by the Gray-Level Co-occurrence Matrix (GLCM) analysis. The input of V-RACNet is the pre-extracted features of GLCM analysis. hese features are further interrogated using V-RACNet with VGG19 layers, which are initially designed to perform image classification.. After VGG19, the features are processed by recurrent layers, in which case, they are LSTMs. The V-RACNet strategic combination of VGG19 and recurrent layers makes the most use of the complementary nature of both spatial and temporal information in detecting and classifying glaucoma.

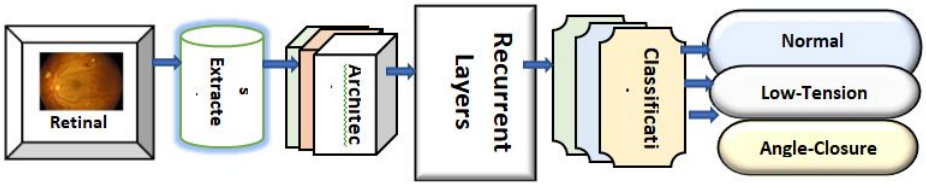

Figure 2: Architecture of the Proposed V-RACNet Model.

FIGURE 2 explains the architecture of V-RACNet Model. The novelties associated with it are that V-RACNet proposes a simplified approach to glaucoma recognition and classification that is based on the utilization of already extracted features along with VGG19 and recurrent layers. Consequently, V-RACNet is an innovative solution of glaucoma detection, which offers a simplified yet efficient approach to exploiting existing features with VGG19 and recurrent layers in fine classification and detection issues.

3.1 Algorithm

This algorithm describes the steps involved in V-RACNet, emphasising its adaptability and robustness.

Algorithm: V-RACNet Model

```
% Step 1: Define V-RACNet Function
function output = V-RACNet(input features)
% Step 2: Extract Spatial Features using VGG19
vgg19_output = VGG19(input features);
% Step 3: Capture Temporal Dynamics using LSTM
lstm_output = LSTM(vgg19_output);
% Step 4: Perform Classification using Dense Layer
output = DenseClassificationLayer(lstm_output); end
% Step 2: Define VGG19 Function
function vgg19_output = VGG19(input features)
% Initialize VGG19 model
vgg19_model = InitializeVGG19();
```

```
% Load pre-trained weights
vgg19_model = loadPretrainedWeights(vgg19_model, 'pretrained_vgg19_weights');
% Pass input_features through VGG19 layers
vgg19_output = vgg19_model(input_features); end
% Step 3: Define LSTM Function
function lstm_output = LSTM(input_features) % Initialize LSTM model
lstm_model = InitializeLSTM(); % Pass input_features through LSTM layers
lstm_output = lstm_model(input_features);
end
% Step 4: Define Dense Classification Layer Function
function output = DenseClassificationLayer(input_features)
% Initialize dense classification layer dense_model = InitializeDenseModel();
% Pass input_features through dense layer
output = dense_model(input_features);
end
```

4. RESULTS AND ANALYSIS

FIGURE 3 illustrates the input image (f(x, y)) which is changed by a number of steps.

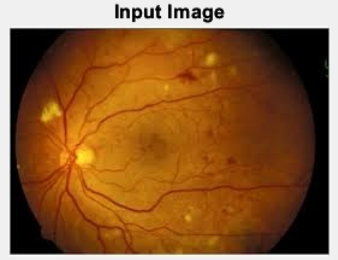

Figure 3: Input Image

The image in the green plane fg (x, Y)) which was derived out of the original input image is represented in FIGURE 4. The green channel information is important in isolating features that are related to blood vessels. The picture is then scaled to 512 by 512 pixels.

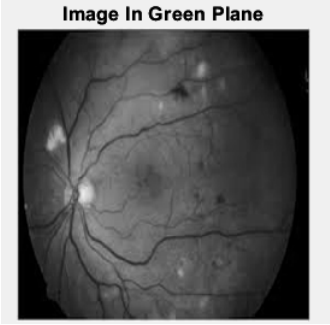

Figure 4: Image in Green plane

FIGURE 5 shows the result of morphological operation of dilation, erosion and thresholding of the image k(x,y) to produce the dilated image ((k(x, y)).

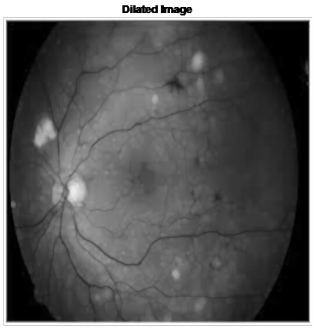

Figure 5: Dilated Image

FIGURE 6 depicts the image of the erosion using morphological operations on the dilated image ((k(x, y))). FIGURE 7 shows the difference image that shows the difference between the dilated and eroded images.

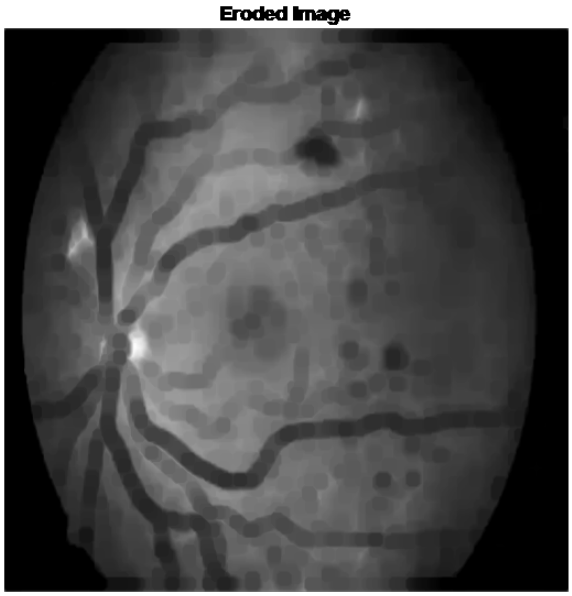

Figure 6: Eroded Image

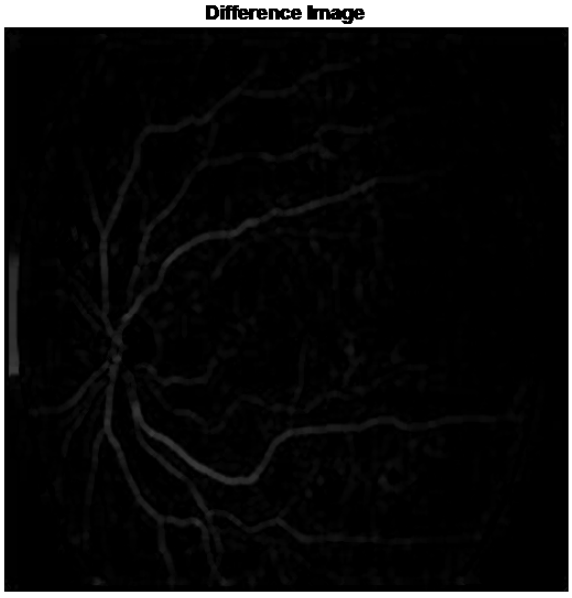

Figure 7: Difference Image

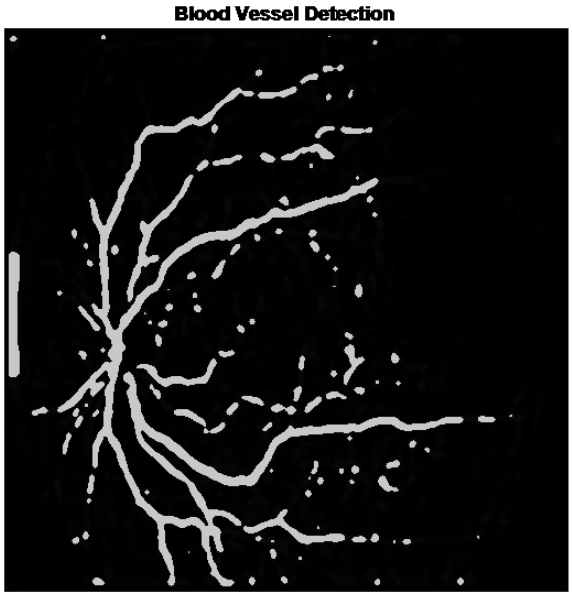

Figure 8: Blood Vessel Detection

FIGURE 8 shows the results of blood vessel detection. The result of morphological operations on the binary image is a FIGURE 9 illustrating the thinned vessels ((l(x, y))) after being thinned.

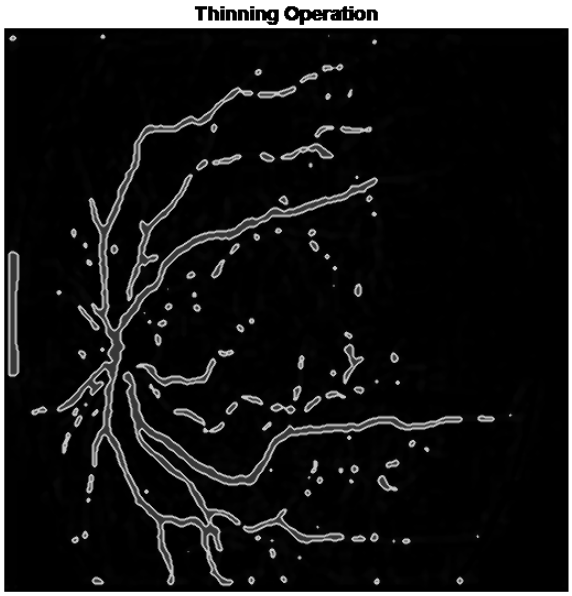

Figure 9: Thinning operated ended Vessels.

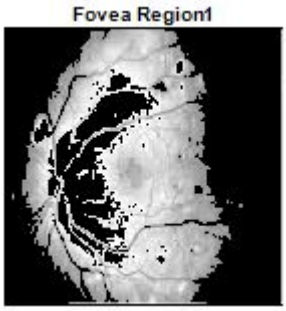

Figure 10: Fovea Region 1

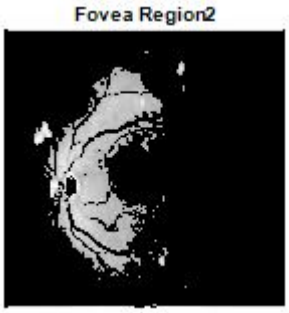

Figure 11: Fovea Region 2

Figure 10 and Figure 11 identify particular areas of interest in the image, which are referred to as Fovea Region 1 and Fovea Region 2. The model of glaucoma detection proposed was also trained on a 1114 samples dataset of the DRIVE database [21], which has 650 normal samples and 464 glaucomatous samples of Low-Tension Glaucoma and Angle-Closure Glaucoma. A detailed set of features derived out of retinal fundus images is presented in TABLE 1.

Table 1: Features extracted for Samples of Retinal fundus Images

Features Extracted	**Sample Retinal Fundus Images**				
	Sample 1	**Sample 2**	**Sample 3**	**Sample 4**	**Sample 5**
Contrast	656.6044	411.5598	648.8319	661.34	653.8215
Correlation	0.8812	0.8843	0.8798	0.8812	0.8816
Energy	0.2577	0.1697	0.1409	0.2217	0.1510
Homogeneity	0.8772	0.8600	0.8586	0.8862	0.8619
Mean	43.8804	32.0898	54.6299	44.3904	55.6134
Entropy	0.9884	0.9765	0.9598	0.9901	0.9610
Decision	**Low-Tension Glaucoma**	**Normal**	**Angle-Closure Glaucoma**	**Low-Tension Glaucoma**	**Angle-Closure Glaucoma**

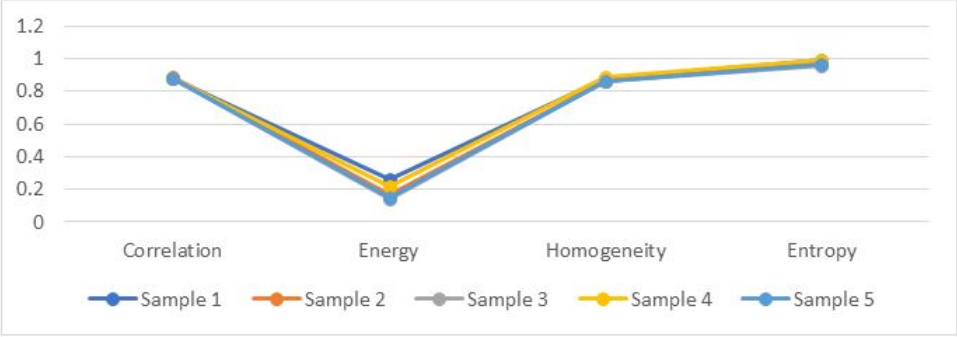

Figure 12: Correlation, Energy, Homogeneity and Entropy features

FIGURE 12 displays the correlation,Energy,Homegeneity and Entropy features. FIGURE 13 is concentrated on the Contrast and Mean features. Contrast is used to determine the difference in pixel intensity between adjacent pixels and this shows the distinctiveness of features of an image. The finding was the increased difference in the types of glaucoma over healthy fundus images, which is similar to the prior results in TABLE 1.

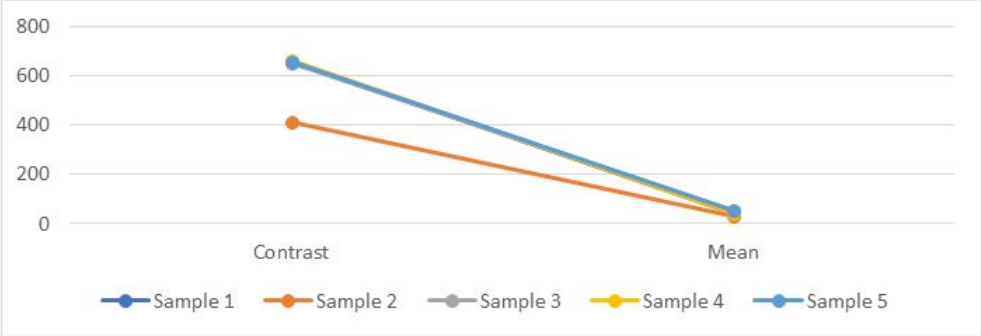

Figure 13: Contrast and Mean Features

To sum up, TABLE 1 and FIGURE 12 and FIGURE 13 reveal that extracted features are important in the separation of healthy and glaucomatous retinal fundus images.

Figure 14: Message Dialogue showing Classified type of Glaucoma

Lastly, FIGURE 14 shows a message conversation representing the categorical type of glaucoma with the trained V-RACNet model. The model is trained over a labelled database which contains the images of normal healthy eyes, low-tension glaucoma and angle-closure glaucoma.

4.1 Accuracy Metric:

The measure of accuracy is the number of correct predictions made as compared to the number of predictions made.

$$accuracy = \frac{(TP\,(class) + TN\,(class))}{TP\,(class) + FP\,(class) + TN\,(class) + FN\,(class)} \tag{17}$$

The TABLE 2, entitled ”Accuracy Analysis” displays the impressive performance of the proposed method of detecting Glaucoma where the accuracy stands at 99.32.

Table 2: Accuracy Analysis

Methods	Accuracy (%)
ResNet-50 [20]	98.48
CNN-based model [22]	96.64
24 Layered CNN architecture [23]	98.6
CNN with Softmax Classifier [24]	95.61
CNN + Adam Optimizer [25]	90.5
Proposed Method	**99.32**

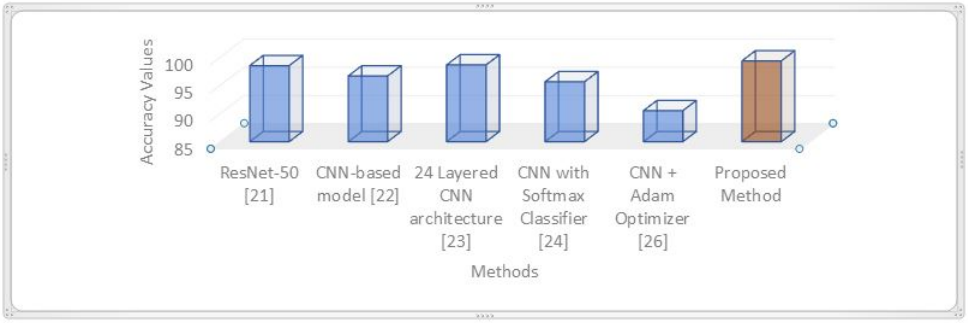

Figure 15: Plot of Comparative Analysis of Accuracy

The relative accuracy of the different methods is shown in FIGURE 15. This level of accuracy is highly important in medical processes, especially in the process of detecting Glaucoma, where, accurate and reliable predictions are necessary in providing an effective treatment of a patient.

4.2 Sensitivity Metric:

It is a significant measure in binary classification issues, especially when the cost of false negatives (missed positive instances) is large and it is expressed as the following equation.

$$sensitivity = \frac{TP\,(class)}{TP\,(class) + FN\,(class)} \quad \ldots\ldots\ldots\ldots\ldots\ldots\ldots\ldots\ldots\ldots\ldots\ldots \quad (18)$$

Table 3: Sensitivity Analysis

Methods	Sensitivity (%)
ResNet-50 [20]	99.30
CNN-based model [22]	96.07
24 Layered CNN architecture [23]	99.40
CNN with Softmax Classifier [24]	89.58
CNN + Adam Optimizer [25]	73
Proposed Method	**99.42**

TABLE 3 that follows, named as Sensitivity Analysis, is a closer look at how the proposed V-RACNet was sensitive in detecting Glaucoma In particular, the sensitivity findings of the suggested approach are contrasted with the ResNet-50 [20], The high sensitivity of 99.42% obtained by the proposed V-RACNet is indicative of the fact that it is highly sensitive to detecting cases of Glaucoma.

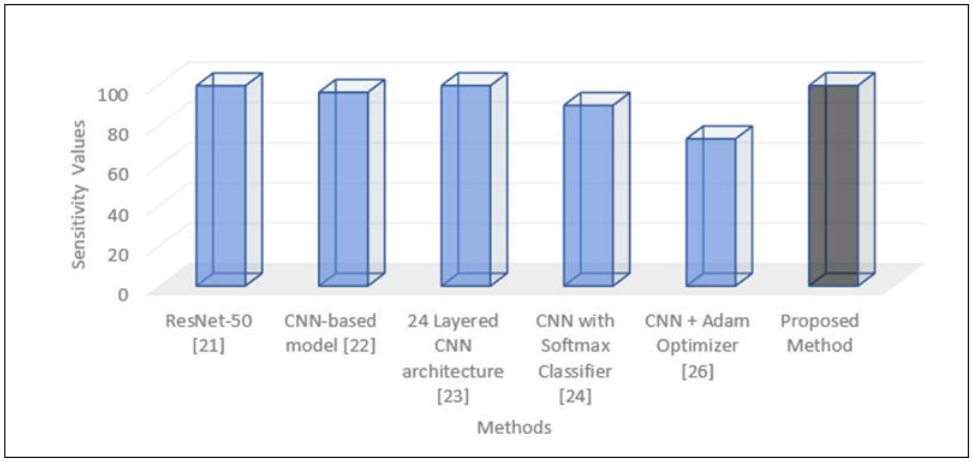

Figure 16: Plot of Comparative Analysis of Sensitivity

FIGURE 16 represents the comparative analysis of senstivity among different methods. The relative accuracy of the different methods is shown in FIGURE 15. This level of accuracy is highly important in medical processes, especially in the process of detecting Glaucoma.

4.3 Specificity Metric:

Specificity assesses the model's capability to appropriately recognize negative instances.

$$specificity = \frac{TN\,(class)}{(FP\,(class) + TN\,(class))} \quad \ldots\ldots\ldots\ldots\ldots\ldots\ldots\ldots\ldots\ldots\ldots\ldots \quad (19)$$

In the TP, True neg, False Positive and False Negative, where TP is True Positive, TABLE 4, entitled as Specificity Analysis, gives a critical analysis of the specificity performance of the proposed method in the detection of glaucoma.

FIGURE 17 represents the comparative analysis of speficivity among different methods. The specificity of 98.58% obtained negative in Glaucoma, which proves it to be an effective tool in the given domain compared to the current methodology.

Table 4: Specificity Analysis

Methods	Specificity (%)
ResNet-50 [20]	96.52
CNN-based model [22]	97.39
24 Layered CNN architecture [23]	97.8
CNN + Adam Optimizer [25]	97.6
Proposed Method	**98.58**

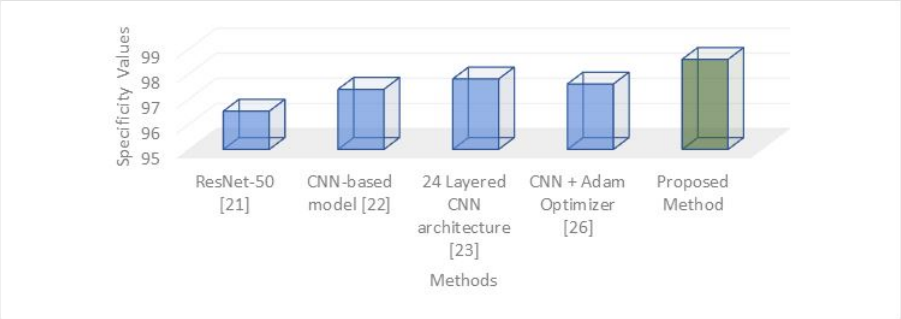

Figure 17: Plot of Comparative Analysis of Specificity

4.4 Precision Metric:

Precision is a measure that determines how the model is able to identify positive instances correctly among the positive instances that the model predicts.

$$Precision = \frac{TN\,(class)}{(TP\,(class) + FP\,(class))} \quad \ldots\ldots\ldots\ldots\ldots\ldots\ldots\ldots\ldots\ldots \quad (20)$$

Table 5: Precision Analysis

Methods	Precision (%)
CNN-based model [22]	97.74
24 Layered CNN architecture [23]	97.8
U-Net [26]	98.4
CNN + Adam Optimizer [25]	96.9
Proposed Method	**99.26**

The results presented in TABLE 5, which is named ”Precision Analysis,” give a scrutiny to the precision performance of the suggested method in the sphere of Glaucoma detecting. The parameter Precision is significant in the medical diagnostics since it determines the positive prediction accuracy of the model. The proposed method has a precision of 99.26, as shown in the table and it is better than the previous works. such as a CNN-based model a 24-layered CNN architecture , U-Net , and CNN with Adam Optimizer [23]. [24] used DRIVE database for Glaucoma related tasks for clinical rationale.

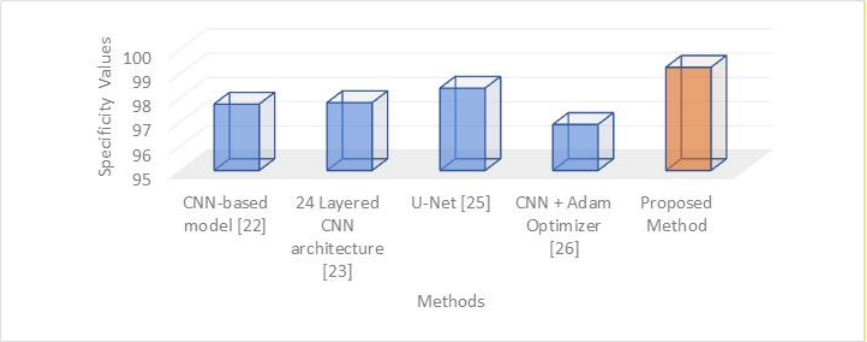

Figure 18: Plot of Comparative Analysis of Precision

Along with the precision analysis, FIGURE 18 represents the comparative analysis of precision of various methods. FIGURE 18 also uses a plot where differentiating small details in the performance would be better presented with precision comparisons of the visualization, and the plot in FIGURE 18 highlights the high level of accuracy of the proposed method. Quantitative values in TABLE 5, and visual data in FIGURE 18 prove that the suggested approach would be effective in providing high accuracy in the glaucoma detection. This makes the proposed method a valid instrument with better positive prediction power than the past methods.

5. CONCLUSION

Conclusively research provides a powerful and holistic pipeline to diagnose glaucoma by processing retinal images. The suggested methodology, comprising image processing, feature extraction and classification with the help of V-RACNet model, proves its effectiveness in the correct recognition of glaucomatous cases. The fact that the model is using a wide range of data of the DRIVE database, including normal and glaucomatous pictures that are further divided into various types, makes the model generalize to the different conditions. The obtained high-performance rates, such as, accuracy 99.32, sensitivity 99.42, specificity 98.58 and precision 99.26 highlight the reliability and accuracy of the proposed solution. The overall robustness is achieved in the training and testing processes, as well as the development and evaluation of the V-RACNet model. The success of the same suggests that it can be a sophisticated and automated glaucoma diagnosis tool that could make major contributions to the medical image analysis to improve the effectiveness of healthcare diagnostics.

References

[1] Flaxman SR, Bourne RR, Resnikoff S, Ackland P, Braithwaite T, et al. Global Causes of Blindness and Distance Vision Impairment 1990-2020: A Systematic Review and Meta-Analysis. Lancet Glob Health. 2017;5:e1221-e1234.

[2] https://www.who.int/publications-detail-redirect/world-report-on-vision

[3] Kumar A, Shaik F, Rahim BA, Kumar DS. Signal and Image Processing in Medical Applications. Heidelberg: Springer. 2016.

[4] Lu W, Tong Y, Yu Y, Xing Y, Chen C, et al. Applications of Artificial Intelligence in Ophthalmology: General Overview. J Ophthalmol. 2018;2018:15.

[5] Akkara JD, Kuriakose A. Role of Artificial Intelligence and Machine Learning in Ophthalmology. Kerala J Ophthalmol. 2019;31:150-160.

[6] Shaik F, Sharma AK, Ahmed SM. Hybrid Model for Analysis of Abnormalities in Diabetic Cardiomyopathy and Diabetic Retinopathy Related Images. SpringerPlus. 2016;5:507.

[7] Stella Mary MC, Rajsingh EB, Naik GR. Retinal Fundus Image Analysis for Diagnosis of Glaucoma: A Comprehensive Survey. IEEE Access. 2016;4:4327-4354.

[8] Senjam SS. Glaucoma Blindness – A Rapidly Emerging Non-Communicable Ocular Disease in India: Addressing the Issue With Advocacy. J Fam Med Prim Care. 2020;9:2200-2206.

[9] Shaik F, Sharma AK, Ahmed SM. Detection and Analysis of Diabetic Myonecrosis Using an Improved Hybrid Image Processing Model. In 2016 2nd International Conference on Advances in Electrical Electronics Information Communication and Bio-Informatics. AEEICB. IEEE. 2016;314-317.

[10] Sarhan A, Rokne J, Alhajj R. Glaucoma Detection Using Image Processing Techniques: A Literature Review. Comput Med Imaging Graph. 2019;78:101657.

[11] Akbar S, Akram MU, Sharif M, Tariq A, Khan SA. Decision Support System for Detection of Hypertensive Retinopathy Using Arteriovenous Ratio. Artif Intell Med. 2018;90:15-24.

[12] Kumar BN, Chauhan RP, Dahiya N. Detection of Glaucoma Using Image Processing Techniques: A Review. In 2016 International conference on microelectronics, computing and communications. MicroCom. IEEE. 2016:1-6.

[13] Ravindraiah R, Reddy SC, Prasad PR. Detection of Exudates in Diabetic Retinopathy Images Using Laplacian Kernel Induced Spatial Fcm Clustering Algorithm. Indian J Sci Technol. 2016;9:1-6.

[14] https://shop.elsevier.com/books/clinical-ophthalmology-international-edition/kanski/978-0-08-045009-4

[15] Schuster AK, Erb C, Hoffmann EM, Dietlein T, Pfeiffer N. The Diagnosis and Treatment of Glaucoma. Dtsch Ärztebl Int. 2020;117:225-234.

[16] Staal J, Abràmoff MD, Niemeijer M, Viergever MA, Van Ginneken B. Ridge-Based Vessel Segmentation in Color Images of the Retina. IEEE Trans Med Imaging. 2004;23:501-509.

[17] Akbar S, Hassan M, Akram U, Yasin UU, Basit I. AVRDB: Annotated Dataset for Vessel Segmentation and Calculation of Arteriovenous Ratio. In Proceedings of the International Conference on Image Processing Computer Vision and Pattern Recognition. IPCV. Las Vegas. 2017:129-134.

[18] Shinde R. Glaucoma Detection in Retinal Fundus Images Using U-Net and Supervised Machine Learning Algorithms. Intell-Based Med. 2021;5:100038.

[19] Sreng S, Maneerat N, Hamamoto K, Win KY. Deep Learning for Optic Disc Segmentation and Glaucoma Diagnosis on Retinal Images. Appl Sci. 2020;10:4916.

[20] Shoukat A, Akbar S, Hassan SA, Iqbal S, Mehmood A, et al. Automatic Diagnosis of Glaucoma From Retinal Images Using Deep Learning Approach. Diagnostics. 2023;13:1738.

[21] Jaya Krishna N, Shaik F, Harish Kumar GC, Naveen Kumar Reddy D, Obulesu MB. Retinal Vessel Tracking Using Gaussian and Radon Methods. In ICCCE 2020: Proceedings of the 3rd International Conference on Communications and Cyber Physical Engineering. Springer Nature. 2021:375-384.

[22] Elangovan P, Nath MK. Glaucoma Assessment From Color Fundus Images Using Convolutional Neural Network. Int J Imaging Syst Technol. 2021;31:955-971.

[23] Bragança CP, Torres JM, Soares CP, Macedo LO. Detection of Glaucoma on Fundus Images Using Deep Learning on a New Image Set Obtained With a Smartphone and Handheld Ophthalmoscope. Healthcare. 2022;10:2345.

[24] Fu Y, Chen J, Li J, Pan D, Yue X, et al. Optic Disc Segmentation by U-Net and Probability Bubble in Abnormal Fundus Images. Pattern Recognit. 2021;117:107971.

[25] Bragança CP, Torres JM, Soares CP, Macedo LO. Detection of Glaucoma on Fundus Images Using Deep Learning on a New Image Set Obtained With a Smartphone and Handheld Ophthalmoscope. Healthcare. 2022;10:2345.

[26] Kashyap R, Nair R, Gangadharan SM, Botto-Tobar M, Farooq S, Rizwan A. Glaucoma Detection and Classification Using Improved U-Net Deep Learning Model. Healthcare. 2022;10, No. 12:2497).